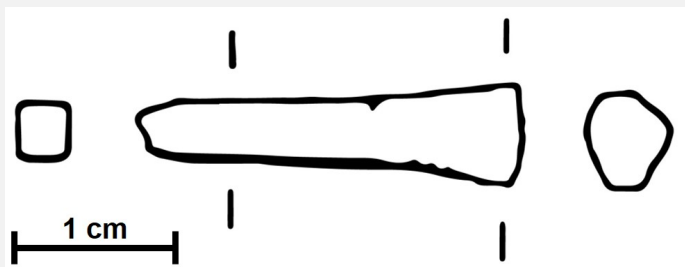


## TANG FRAGMENT OF A KNIFE HR-6567 - LEADED BRONZE - LATE BRONZE AGE - SWITZERLAND

<b>Artefact name</b>	Tang fragment of a knife HR-6567
<b>Authors</b>	Marianne. Senn (Empa, Dübendorf, Zurich, Switzerland) & Christian. Degrigny (HE-Arc CR, Neuchâtel, Neuchâtel, Switzerland) & Naima. Gutknecht (HE-Arc CR, Neuchâtel, Neuchâtel, Switzerland) & Rémy. Léopold (HE-Arc CR, Neuchâtel, Neuchâtel, Switzerland)
<b>Url</b>	/artefacts/1364/

∨ The object



Credit Laténium.

Fig. 1: Tang fragment of a knife (after Rychner-Faraggi 1983, plate 35.26),



Fig. 2: Dense and brown-yellow corrosion product (detail) of the tang fragment of a knife,

Credit HE-Arc CR, N.Gutknecht/L.Rémy.

Description and visual observation

<b>Description of the artefact</b>	Fragment de Tang avec des produits de corrosion brun-jaune brillants encore en place localement (Fig. 2). Dimensions : L = 2,9 cm ; Ømax. = 6,8 mm ; WT = 4,9 g.
<b>Type of artefact</b>	Household implement
<b>Origin</b>	Hauterive - Champréveyres, Neuchâtel, Neuchâtel, Switzerland
<b>Recovering date</b>	Excavation in 1983-1985, layer 3
<b>Chronology category</b>	Late Bronze Age
<b>chronology tpq</b>	1054 B.C. ▾
<b>chronology taq</b>	1000 B.C. ▾
<b>Chronology comment</b>	Hallstatt B1 (1054/1037BC _ 1000BC)
<b>Burial conditions / environment</b>	Lake
<b>Artefact location</b>	Laténium, Neuchâtel, Neuchâtel
<b>Owner</b>	Laténium, Neuchâtel, Neuchâtel
<b>Inv. number</b>	HR-6567
<b>Recorded conservation data</b>	No conservation data available, but a coating and inventory number is visible on the surface.

Complementary information

L'objet a été échantillonné en 1987 pour analyse. La documentation des strates en mode binoculaire sur le fragment restant de l'objet a été réalisée en 2022.

Study area(s)

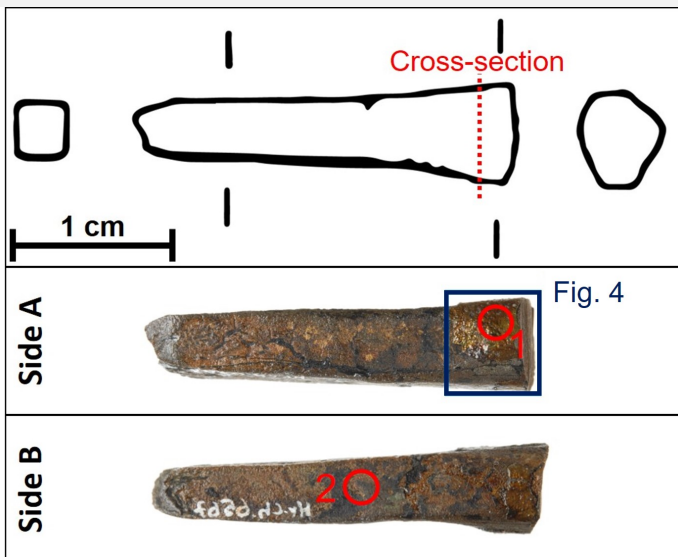
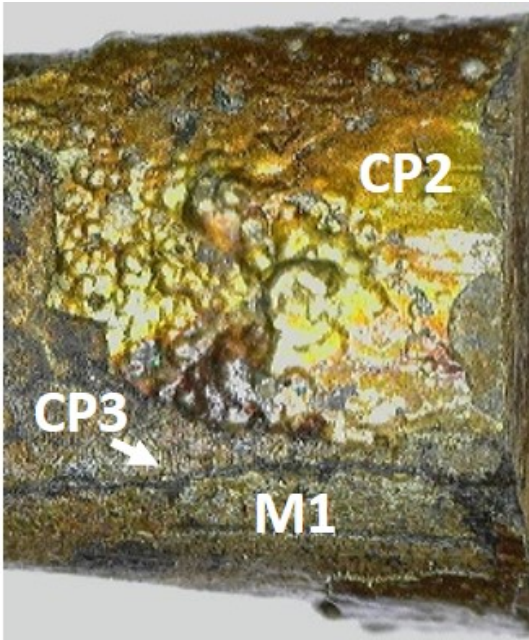


Fig. 3: Location of cross-section on drawing before sampling and both sides of fragment (after sampling) with location of the detail of Fig. 4 and XRF analysis areas (red circles),

Credit HE-Arc CR, N.Gutknecht/L.Rémy.

Fig. 4: Corrosion structure (detail) from Fig. 3 showing some of the documented strata in Fig. 5,



Credit HE-Arc CR, N.Gutknecht.

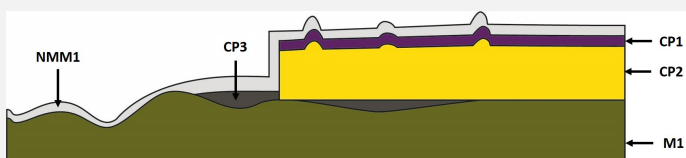
✧ Binocular observation and representation of the corrosion structure

La représentation schématique ci-dessous donne un aperçu de la structure de corrosion rencontrée sur le fragment à partir d'une première observation macroscopique visuelle.

Couches	Type de strate	Principales caractéristiques
NMM1	Matériau non métallique	Film/revêtement, transparent, mince, continu
CP1	Produit corrosif	Brun, nacré, fin, discontinu, compact
CP2	Produit corrosif	Jaune foncé, épais, discontinu, compact, dur
CP3	Produit corrosif	Layer, dark grey, thin, scattered, non-compact, soft
M1	Metal	Olive, thick, metallic, soft

Table 1: Description of the principal characteristics of the strata as observed under binocular and described according to Bertholon's method.

The NMM1 seems to be a polymer coating added after excavation of the object.

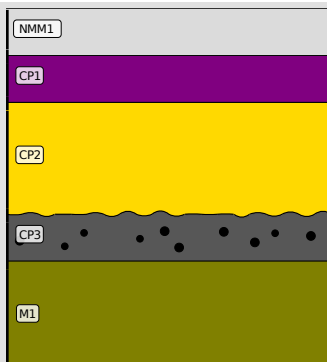


Credit HE-Arc CR, N.Gutknecht.

Fig. 5: Stratigraphic representation of the corrosion structure of the tang of a knife by macroscopic and binocular observation with reference to Fig. 4,

✧ MiCorr stratigraphy(ies) – Bi

Fig. 6: Stratigraphic representation of the corrosion structure of the tang of a knife observed macroscopically under binocular microscope using the MiCorr application with reference to the whole Fig. 5. The characteristics of the strata, such as discontinuity, are accessible by clicking on the drawing that redirects you to the search tool by stratigraphy representation, Credit HE-Arc CR, N.Gutknecht.



Sample(s)

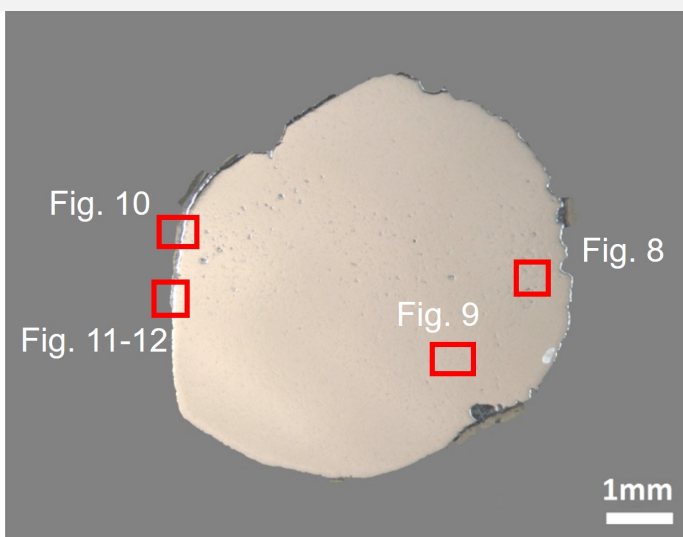


Fig. 7: Micrograph of the cross-section of the sample taken from the tang fragment of a knife showing the location of Figs. 8 to 12,

Credit HE-Arc CR.

<b>Description of sample</b>	This cross-section shows a lateral cut through the tang (Fig. 3). Most of the corrosion structure is absent (Fig. 7).
<b>Alloy</b>	Leaded Bronze
<b>Technology</b>	Cold worked with partial annealing
<b>Lab number of sample</b>	MAH 87-196
<b>Sample location</b>	Musées d'art et d'histoire, Genève, Geneva
<b>Responsible institution</b>	Musées d'art et d'histoire, Genève, Geneva
<b>Date and aim of sampling</b>	1987, metallography and corrosion characterisation

Complementary information

None.

Analyses and results

*Analyses performed:*

**Non-invasive approach**

XRF with handheld portable X-ray fluorescence spectrometer (NITON XL5). General Metal mode, acquisition time 60s (filters: Li20/Lo20/M20).

**Invasive approach (on the sample)**

Metallography (etched with ferric chloride reagent), Vickers hardness testing, ICP-OES, SEM/EDS (conditions provided in the About tab of the MiCorr application), XRD.

Non invasive analysis

XRF analyses of the tang fragment of a knife were carried out on two representative areas (Fig. 3). Point 1 was done on the dark yellow corrosion layer (CP2), while point 2 was performed on the remaining metal surface. For both points, soil, corrosion products and metal are analyzed at the same time.

The metal is presumably a tin bronze alloy. The other elements detected are: Fe, S, Pb, Si, Al, Sb, As, Co, Ag, Zn.

Results of point 1 are very different from those of point 2, they indicate the enrichment in Fe and in S and depletion in Cu.

Elements (mass %)	Cu		Fe		S		Sn		Pb		Si		Al		Sb		As		Co		Ag		Zn		Total
	%	+/-2σ	%	+/-2σ	%	+/-2σ	%	+/-2σ	%	+/-2σ	%	+/-2σ	%	+/-2σ	%	+/-2σ	%	+/-2σ	%	+/-2σ	%	+/-2σ	%	+/-2σ	
1	37.0	0.1	32.0	0.09	23.5	0.08	4.0	0.02	<0.1	0.01	1.5	0.06	0.5	0.1	0.4	0.01	0.2	0.01	0.2	0.04	0.1	0.01	<0.1	0.02	99
2	77.0	0.1	1.0	0.02	3.5	0.03	9.0	0.04	2.0	0.03	2.0	0.05	0.5	0.1	0.7	0.02	2.0	0.04	0.2	0.01	0.3	0.01	<0.1	0.02	99

Table 2: Chemical composition of the surface of the tang at two representative areas shown in Fig. 3. Method of analysis: XRF, UR-Arc CR.

Metal

The remaining metal is a leaded bronze (Table 2) containing numerous copper sulphide and tiny Pb inclusions (Figs. 8-10, 12 and Table 4). The porosity within the metal is high, particularly along a band through the middle of the sample (Figs. 7 and 8). The etched structure of the leaded bronze shows small, regular polygonal grains, some with twinning (Fig. 9). Slip lines appear in grains close to the metal surface (Fig. 9). The average hardness of the metal is HV1 120.

Elements	Cu	Sn	Pb	Ni	Sb	As	Co	Ag	Fe	Zn
mass%	87.52	8.02	1.46	1.04	0.81	0.60	0.24	0.21	0.05	0.03

Table 3: Chemical composition of the metal. Method of analysis: ICP-OES, Laboratory of Analytical Chemistry, Empa.

Elements	O	S	Fe	Cu	Total
mass%	1.5	20	1.0	71	93

Table 4: Chemical composition of dark-grey inclusions. Method of analysis: SEM/EDS, Laboratory of Analytical Chemistry, Empa.

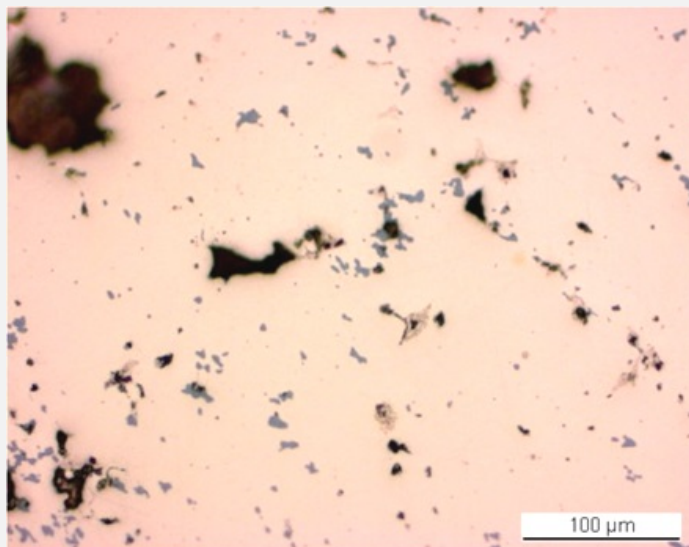


Fig. 8: Micrograph of the metal sample from Fig. 7 (detail), unetched, bright field. In pink the metal, in black the porosity and in dark-grey copper sulphide inclusions,

Credit HE-Arc CR.

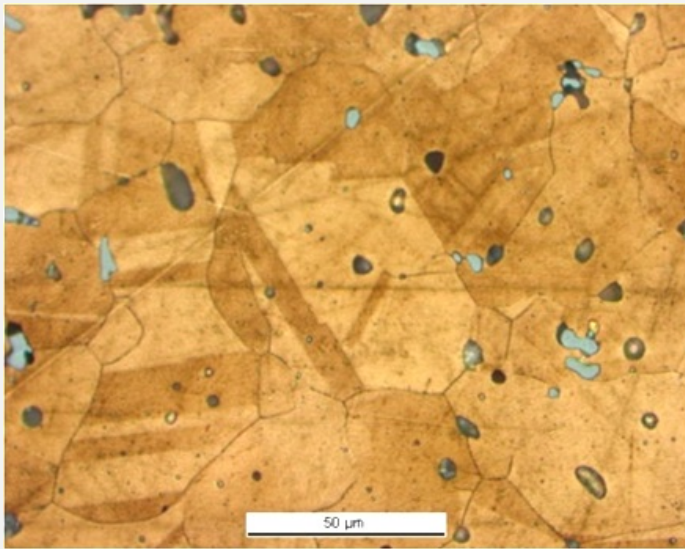


Fig. 9: Micrograph of the metal sample from Fig. 7 (detail), etched, bright field. Angular and twinned grains are revealed as well as copper sulphide inclusions in grey,

Credit HE-Arc CR.

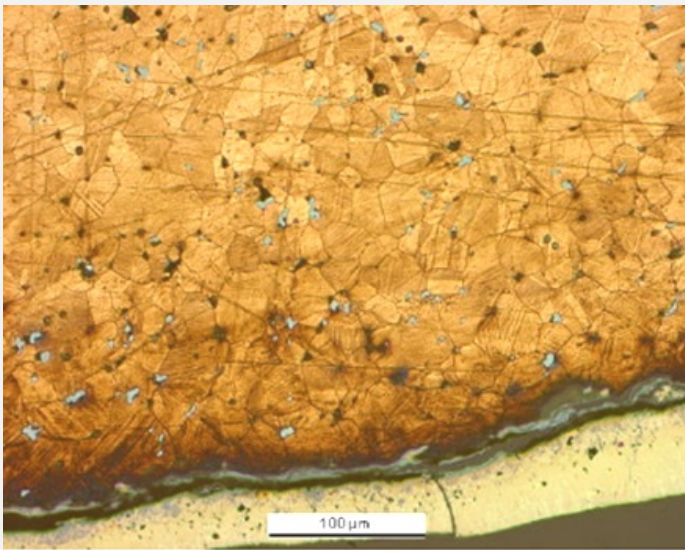


Fig. 10: Micrograph of the metal sample from Fig. 7, etched, bright field (rotated by 270°, detail). Angular grains with slip lines can be seen as well as copper sulphide inclusions in grey,

Credit HE-Arc CR.

<b>Microstructure</b>	Polygonal and twinned grains + strain lines (metal surface) with pores
<b>First metal element</b>	Cu
<b>Other metal elements</b>	Co, Ni, As, Ag, Sn, Sb, Pb

**Complementary information**

None.

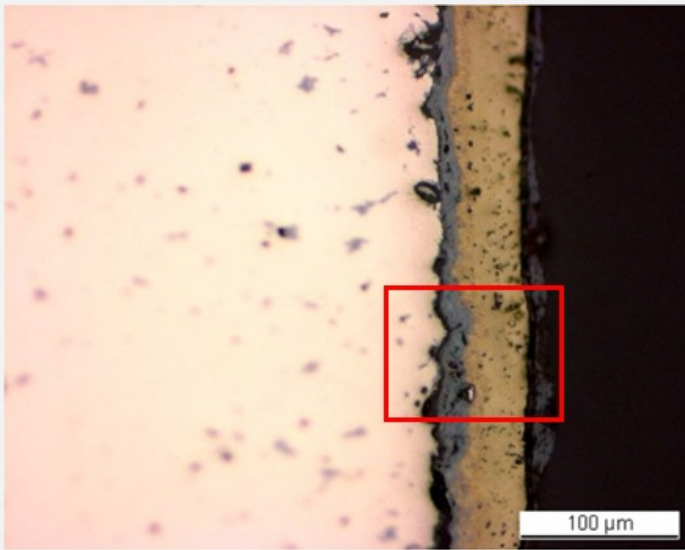
⌵ Corrosion layers

The metal has lost most of its original corrosion layer, the remainder having an average thickness between 60 and 190µm (Fig. 6). In some areas up to three corrosion strata are visible (Fig. 11). In polarised light (Fig. 12), the corrosion stratigraphy appears more clearly: it is composed of a dense black inner layer, an intermediate thick brown layer with bright spots (indicating porosity) and an outer red layer with white particles. The elemental chemical distribution of the SEM image reveals that the black inner layer (CP3) is Sn-rich, but contains Cu, O, Fe, Si, P, Pb, Ni, As, Ca and S (Table 5, Figs. 12-13). The brown layer (CP2) contains S, Fe and Cu and has a composition similar to chalcopyrite/CuFeS<sub>2</sub> (Table 5, Figs. 12-13). This was confirmed by past XRD analyses carried out by Schweizer (1994, museum report (1987)). The red layer (CP1) is an iron oxide (main elements Fe and O) and is contaminated with calcite/CaCO<sub>3</sub> particles (S1) (Table 5, Figs. 12-13).

Elements	O	Fe	Ni	Cu	Si	P	S	Ca	As	Sn	Pb	Total
<b>CP1, red layer</b>	37	51	1.8	<	<	<	<	2	1	<	<	<b>93</b>
<b>CP2, brown layer</b>	<	30	<	42	<	<	35	<	<	<	<	<b>107</b>

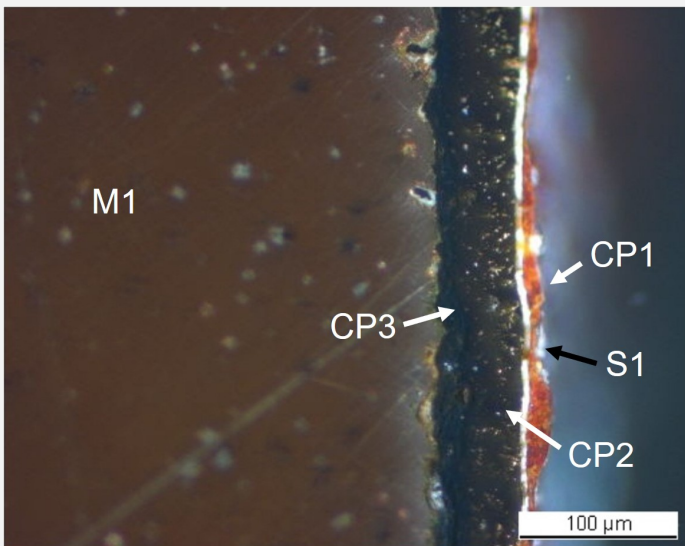
CP2, white particles	50	<	<	<1	<	<	<	39	<	<	<	90
CP3, black layer	39	5	1	5	4	4	<	<	<1	37	4	100

Table 5: Chemical composition (mass %, <: below the detection limit) of the corrosion layers (from Figs. 12). Method of analysis: SEM/EDS, Laboratory of Analytical Chemistry, Empa.



Credit HE-Arc CR.

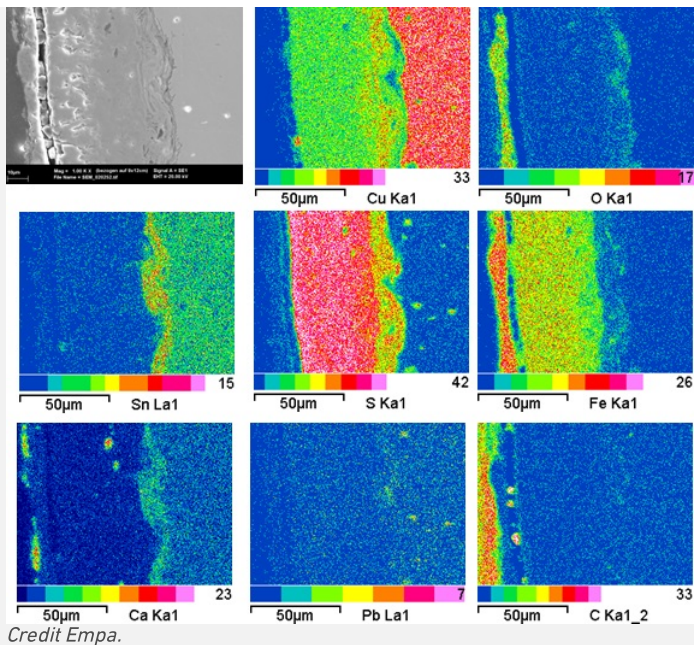
Fig. 11: Micrograph of the metal sample from Fig. 7 (reversed picture, detail), unetched, bright field. From left to right: metal (in pink), inner light-grey layer, intermediate brown layer and top dark-grey layer. The area selected for elemental chemical distribution (Fig. 13) is marked by a red rectangle,



Credit HE-Arc CR.

Fig. 12: Micrograph of the same area as Fig. 11 and corresponding to the stratigraphy of Fig. 14, polarized light. From left to right: metal (in brown) covered with a corrosion layer consisting of a black layer, an intermediate brown layer with bright spots, a crack (white line) and a red layer with white particles,

Fig. 13: SEM image, SE-mode, and elemental chemical distribution of the selected area of Fig. 11 (reversed picture). Method of examination: SEM/EDS, Laboratory of Analytical Chemistry, Empa,



Credit Empa.

Corrosion form                      Uniform  
 Corrosion type                      lake patina (Schweizer 1994)

Complementary information

None.

∨ MiCorr stratigraphy(ies) – CS

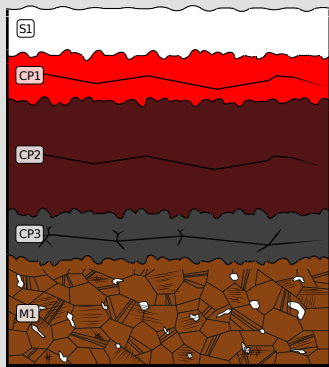


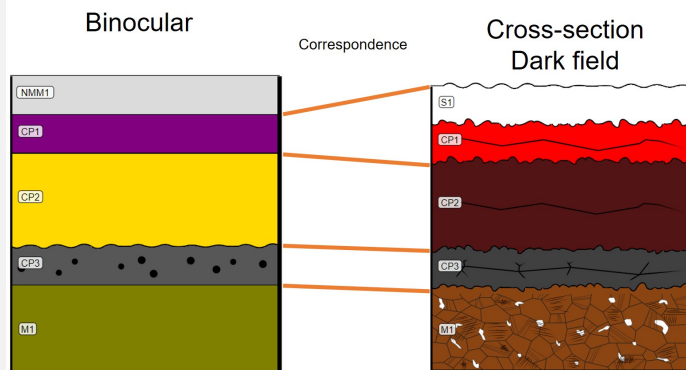
Fig. 14: Stratigraphic representation of the sample taken from the tang fragment of a knife in cross-section (dark field) using the MiCorr application. The characteristics of the strata are accessible by clicking on the drawing that redirects you to the search tool by stratigraphy representation. This representation can be compared to Fig. 12, Credit HE-Arc CR.

∨ Synthesis of the binocular / cross-section examination of the corrosion structure

NMM1 in binocular mode is not observed in cross-section mode, as the cross-section does not show any coating.  
 CP1 in binocular mode is documented as sediment (S1) and CP1 in cross-section mode. But it is not clear if it matches the CP1 from cross-section, which is a Fe-rich layer, or if CP1 from binocular mode developed as an atmospheric corrosion after the excavation and is therefore not present on the embedded sample.  
 CP2 and CP3 in binocular mode match CP2 and CP3 in cross-section mode.  
 On cross-section, it was possible to describe and analyze the microstructure of the metal.

Fig. 15: Stratigraphic representation side by side of binocular view and cross-section (dark field),





Credit HE-Arc CR, N.Gutknecht/L.Rémy

## Conclusion

The tang fragment is made from a leaded bronze and has been cold worked on the top surface after annealing. The SEM/EDS examination and past XRD analyses indicate the presence of chalcopryite in the corrosion layer, typical of lake context (Schweizer 1994). This corrosion layer is enriched with Sn close to the metal surface and depleted of Cu on the outer surface. The limit of the original surface most probably lies between the Sn-rich inner layer and the Fe and S-rich outer layers. The presence of iron oxides on top of the copper corrosion layer has not yet been explained. The corrosion is a type 1 according Robbiola et al. 1998.

Cet objet a été échantillonné pour la première fois en 1987. Grâce à une importante documentation sur coupe et comparaison avec des objets similaires (voir références), Schweizer définit sur cet objet une typologie "patine lacustre" qui renseigne sur l'environnement de la sépulture. En effet, selon ses recherches, la « patine lacustre » dense, analysée comme de la chalcopryite, ne peut être générée qu'en présence de bactéries sulfato-réductrices. Les conditions pour ces bactéries sont un environnement anaérobie, humide et riche en S et Fe. Cet objet a probablement été abandonné directement dans le lac

## References

### Références sur l'objet et l'échantillon

#### Fichiers objet dans MiCorr

1. MiCorr\_Pin ou fragment d'aiguille HR-3031
2. MiCorr\_Tang fragment d'un couteau HR-6246
3. MiCorr\_Pin HR-18152
4. MiCorr\_Pin HR-17773
5. MiCorr\_Pin HR-3071
6. MiCorr\_Pin HR-18603
7. MiCorr\_Pin HR-3389

#### Objet Références

8. Rychner-Faraggi AM. (1993) Hauterive – Champprévèyres 9. Métal et parure au Bronze finale. Archéologie neuchâteloise, 17 (Neuchâtel).
9. Hochuli, S. et al. (1988) SPM III Bronzezeit, Verlag Schweizerische Gesellschaft für Ur- und Frühgeschichte Basel, 76-77, 379.

#### Échantillon de références

10. Rapport Empa 137 695/1991, PO Boll.
11. Rapport d'examen, Lab. Musées d'Art et d'Histoire, Genève GE, 87-194 à 87-197.
12. Schweizer, F. (1994) Objets en bronze des sites lacustres : de la patine à la bibliographie. Dans : Métaux anciens et historiques, conservation et recherche scientifique (eds. Scott, DA, Podany, J. et Considine BB), The Getty Conservation Institute, 33-50.

### Références sur les méthodes analytiques et l'interprétation

13. Robbiola, L., Blengino, JM., Fiaud, C. (1998) Morphologie et mécanismes de formation des patines naturelles sur les alliages Cu-Sn archéologiques, Corrosion Science, 40, 12, 2083-2111.